REGULAR ARTICLE

A DFT study of uracil and 5-bromouracil in nanodroplets

Tanja van Mourik · Victor I. Danilov ·
Vladimir V. Dailidonis · Noriyuki Kurita ·
Hajime Wakabayashi · Takayuki Tsukamoto

Abstract The canonical (keto) and rare (enol) tautomers of uracil and 5-bromouracil in clusters comprising 50 and 100 water molecules (nanodroplets) were studied using density functional theory. The geometries of the various complexes were optimized at two different levels of theory, BLYP/6-31G(d,p) and B3LYP/6-31G(d,p). Tautomerization energies were computed using the BLYP, B3LYP and M05-2X density functionals. The gas-phase tautomerization energies of uracil and 5-bromouracil are very similar, favoring the keto tautomer. However, in the hydrated phase, the tautomeric preference of 5-bromouracil is reversed. This result is obtained for all four sets of clusters (BLYP or B3LYP optimized, containing 50 or 100 water clusters) and at all levels of theory employed, and indicates that a bromine atom in the 5-position considerably increases the proportion of the hydroxyl group present in uracil.

Keywords Mutagenicity · Uracil · 5-Bromouracil · Water cluster · DFT · Tautomerization

Dedicated to Professor Sándor Suhai on the occasion of his 65th birthday and published as part of the Suhai Festschrift Issue.

T. van Mourik (✉)
School of Chemistry, University of St. Andrews, North Haugh,
St. Andrews, Fife KY16 9ST, Scotland, UK
e-mail: tanja.vanmourik@st-andrews.ac.uk

V. I. Danilov
Department of Molecular and Quantum Biophysics,
Institute of Molecular Biology and Genetics,
National Academy of Sciences of Ukraine,
150 Zabolotny Street, 03143 Kyiv-143, Ukraine

V. V. Dailidonis
Bogolyubov Institute for Theoretical Physics,
National Academy of Sciences of Ukraine,
14b Metrologichaskaya Street, 03143 Kyiv-143, Ukraine

N. Kurita · H. Wakabayashi · T. Tsukamoto
Department of Knowledge-based Information Engineering,
Toyohashi University of Technology, Tempaku-cho,
Toyohashi 441-8580, Japan

1 Introduction

Mutations are changes in the nucleotide sequence of the genetic material (DNA or RNA), which can result in the modification of the amino acid sequence of the protein encoded by the gene. The vast majority of mutations do not affect the fitness of the organism; moreover, DNA repair mechanisms can reverse many changes before they become permanent mutations. However, some mutations do have an effect on the organism's fitness, and these are believed to be the underlying mechanism of natural selection.

In general, the fidelity of the translation of the nucleic acids is maintained by specific Watson–Crick hydrogen bonds (H-bonds) between bases on opposite strands in the DNA double helix. In the canonical DNA structure, adenine (A) binds to thymine (T) and cytosine (C) binds to guanine (G). Uracil (U) takes the place of thymine in RNA. The incorporation of unusual bases or base analogs into the DNA structure may cause spontaneous mutations. For example, the nonstandard nucleic acid base 5-bromouracil (5BrU) acts as a thymine base analog in DNA and can induce DNA mutation. Generally, uracil occurs in the keto form in the double helix [1], but it may also exist in other noncanonical tautomeric forms [2–9]. Freese [10] suggested that the mutagenic activity of 5BrU originates from

the existence of enol tautomers of 5BrU. The existence of such tautomers is supported by experimental results that show that a bromine in the 5-position considerably increases the acidity of the uracil and the proportion of the enol tautomer present in 1-methyluracil [11]. Hu et al. [12] have used the presumed existence of 5BrU enol tautomers to hypothesize a mechanism for the mutagenic activity of 5BrU, which mutates G–C to A–T and A–T to G–C (see Fig. 1). According to this mechanism, the substitution of T by 5BrU in an A–T base pair is followed by keto → enol tautomerization of 5BrU leading to an A-5BrU(enol) base pair. As 5BrU(enol) prefers to pair with G [13], replication produces an A–T and G-5BrU(enol) base pair. In the next replication cycle the G-5BrU(enol) base pair replicates into G–C and G-5BrU(enol) base pairs, completing the mutation from A–T to G–C. Tautomerization of G-5BrU(enol) to G(enol)-5BrU yields G(enol)-T and A-5BrU base pairs, which are repaired to A–T by DNA repair mechanisms, and this route therefore does not lead to mutation.

In the current paper, we focus on the tautomerization step from 5BrU(keto) to 5BrU(enol), and do not consider the other crucial steps in the mutagenic mechanism proposed by Hu et al. If the proposed mechanism is valid, then the tautomerization must be easier for 5BrU than for U. Several studies found that the tautomerization process is highly unfavorable in the gas phase for both U and 5BrU [7, 8, 12, 14–16]. Hu et al. [12, 17] studied the effect of water on the tautomerization energies of U and 5BrU. They distinguished two different water-binding regions, labeled S1 and S2. S1 is the region separated from other regions by lines going through the N3–H and C4=O bonds and S2 is the region between lines through the C5–H (or C5–Br) and C4=O bonds (see Fig. 2 for the atom labeling). A water molecule located in S1 increases the stability of the enol tautomers of U and 5BrU, whereas a water molecule located in S2 decreases it. Thus, water molecules in the S2 region
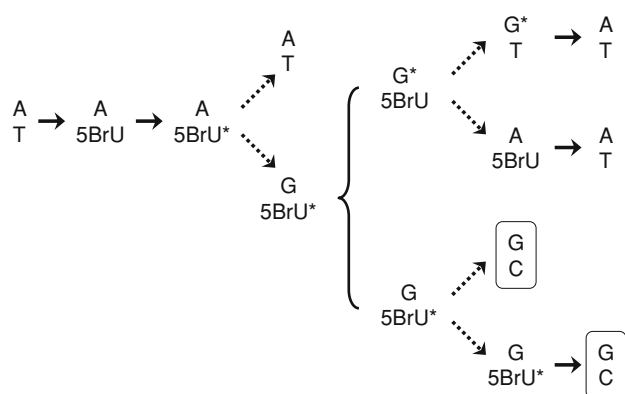
apparently protect the base from tautomerizing to the enol form. As the presence of the bromine atom in 5BrU prevents water from entering the S2 region, the protection induced by water molecules in this region is prohibited in 5BrU. Hu et al. [12] concluded that 5BrU is, therefore, more likely to form an enol tautomer than U, an assumption required for the proposed keto → enol tautomerization mutation mechanism. Additional results obtained by Hu et al. strengthening the proposed mechanism are (1) that 5BrU(enol) prefers to pair with G rather than A, (2) that G-5BrU(enol) and G(enol)-5BrU have similar stabilities, so that the probability of forming a G-5BrU(enol) base pair is sufficiently high. If this would not be the case, then tautomerization to GC would not occur (see Fig. 1). The tautomerization mechanism was, however, deemed unlikely by Hobza et al. [15], primarily on the basis of free-energy calculations in the gas-phase, a single-water hydrated environment and bulk water (modeled by a continuum solvation method). In all three environments the keto tautomer of both U and 5BrU is strongly favored over the enol form. Hobza et al. considered several different singly-hydrated U and 5BrU structures and found that the water molecule only has a small effect on the energy difference between the keto and enol tautomers. In addition, the interaction energy was computed to be larger for the keto form of U than the corresponding 5BrU tautomer when a water molecule was placed in the S2 region, countering Hu et al.'s finding that the presence of a bromine atom in 5BrU prevents water from entering this region. Some of the results obtained by Hu et al. were computed at the rather limited HF/STO-3G level of theory, and may therefore not be reliable. Higher-level calculations conducted by Hobza et al. [15], employing B3LYP/6-31G(d,p) and MP2/6-31G(d,p) calculations at B3LYP/6-31G(d,p) optimized geometries, indicate that the G(enol)-5BrU base pair is preferred over the G-5BrU(enol) base pair, which would mean that the conversion to G–C does not happen. The tautomeric preference of the G-5BrU base pair, however, seems to be dependent on the particular level of theory employed (B3LYP vs. MP2; gas phase vs. hydrated environment), though the best calculations by Hobza et al. [15]

Fig. 1 The keto → enol tautomerization mechanism of 5BrU mutagenicity proposed by Hu et al. [12]. The *asterisk* indicates the enol tautomeric form. The *dashed lines* represent DNA replication. The *boxed base pairs* indicate mutation
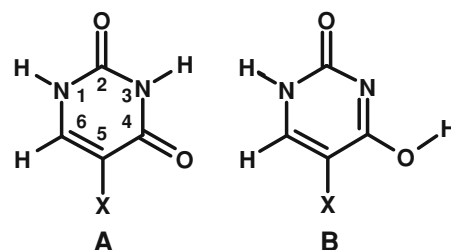

Fig. 2 The canonical keto (a) and rare enol (b) tautomers of uracil (X = H) and 5-bromouracil (X = Br)

[employing relative free energies in water calculated at the MP2/6-31G(d,p)//B3LYP/6-31G(d,p) level] indicate a preference for the G(enol)-5BrU base pair. This result is in agreement with MP2/6-31G(d,p) optimized results in vacuo conducted by two of us [18], which also showed that the G-5BrU(enol) base pair is energetically less favorable than the G(enol)-5BrU base pair. As the keto → enol tauto-merization of 5BrU is the critical step in the proposed mutation mechanism, the conclusion by Hobza et al. that the probability of the enolization process is essentially negli-gible appears to be a strong argument against this mutation model.

However, continuum solvation models, as used in the work by Hobza et al., neither describe the explicit inter-actions between the water molecules and the solute nor those between the water molecules themselves, which may be important to reliably describe the tautomeric preferences of U and 5BrU. In addition, continuum solvation models are known to miss some of the microscopic processes induced by solvation, such as charge transfer. On the other hand, when using models that include explicit water molecules one is faced with the challenges of including a sufficiently large number of water molecules to describe bulk water. Previous calculations on uracil and thymine complexes comprising 11 water molecules [19] and cyto-sine and adenine complexes comprising 14 and 16 water molecules, respectively [20], indicated that the limited-size water clusters used in these calculations do not accurately model bulk water. Thus, larger water clusters are required to obtain reliable results. A recent molecular dynamics study of RNA base pairs in a nanodroplet showed that base pairs exist at a stability minimum when solvated in between 20 and 100 water molecules, and that the stability of RNA base pairs observed in bulk water was reproduced as the number of water molecules increased above 100 [21]. For single bases the number of water molecules required to mimic bulk water is expected to be much smaller, and in initial research on the hydration of U and 5BrU we employed water clusters consisting of 50 water molecules [22]. For the alanine amino acid, this cluster size was found to accommodate two hydration shells [23], and should, therefore, be sufficient to approach the bulk water limit. In our work employing clusters comprising 50 water molecules it was found that the tautomeric preference of 5BrU is greatly affected by aqueous hydration; the pres-ence of the shell of explicit water molecules reverses the tautomeric preference of 5BrU, rendering the rare tautomer to be preferred over the canonical form in aqueous solu-tion. In the current study, even larger water clusters (con-sisting of 100 water molecules) were employed, and the formation energies of the hydrated complexes of the keto and enol tautomeric forms of U and 5BrU were determined at several different levels of theory. Even though the details of the interactions in the complexes differ between the two cluster sizes and depend on the calculation method employed, the basic conclusion remains the same; in aqueous solution, the rare tautomer of 5BrU is preferred over the canonical form.

2 Theoretical calculations

2.1 Geometry optimization

In the current work, the geometry optimizations of the keto and enol forms of U and 5BrU in nanodroplets consisting of 50 or 100 water molecules were carried out at the density functional theory (DFT) level employing the BLYP [24, 25] and B3LYP [24–27] functionals and the 6-31G(d,p) basis set. The enol tautomer considered is the one where the hydrogen attached to N3 in the canonical form has trans-ferred to the O4 oxygen atom (see Fig. 2), as this tautomer can be built into DNA and RNA without significant dis-tortion; it is essentially a cytosine analog, which can bind with guanine through three strong hydrogen bonds. To obtain the optimized structures of the various complexes, the following steps were followed. First, Monte–Carlo (MC) simulations of the bases in the presence of 400 water molecules were performed in the canonical (NVT) ensem-ble using Metropolis sampling [28]. The MC simulations were performed employing the physical cluster theory [29, 30] at 298 K with the aim to obtain reasonable starting structures for the DFT calculations, with an equal distri-bution of water molecules around the base. The simulations employed the refined semiempirical potential functions suggested by Poltev and colleagues [31–33]. The statistical error (dispersion value) was calculated with a precision of ±0.005. Complexes with favorable (e.g., H-bonded) ori-entations of the water molecules were then used to obtain starting structures for the DFT calculations. The 50 or 100 water molecules closest to the center-of-mass of the base were selected and the resulting complexes were first opti-mized with DMol [34], using the BLYP functional and a DNP (double numerical plus polarization) basis set. Numerical basis sets are more effective for the optimization of large systems [35, 36], and the DMol calculations enabled us to get close to the optimal structure of the minima considered within a reasonable time. The geometry optimizations were then continued with Gaussian [37] at the BLYP/6-31G(d,p) and B3LYP/6-31G(d,p) levels of theory. An assessment of a range of density functionals for the prediction of the geometries and relative energies of water hexamers showed that all density functionals tested (which included B3LYP) could reproduce the MP2 geometries well [38], and we, therefore, expect B3LYP to yield reasonable geometries for the hydrated clusters of U and 5BrU.

2.2 Calculation of the formation energies

The formation energies were computed at the BLYP/6-31G(d,p), B3LYP/6-31G(d,p), B3LYP/6-31++G(d,p) and M05-2X/6-31G(d,p) levels of theory, using the BLYP/6-31G(d,p) and B3LYP/6-31G(d,p) optimized geometries. Our choice of functionals was stimulated by the following considerations. M05-2X [39] is a highly parameterized meta-hybrid density functional designed to yield broad applicability in chemistry. It has been shown to give much improved results for noncovalent as well as dispersion-dominated interactions [40–44], and was among the functionals that yielded the most accurate energies for water hexamers [38]. M05-2X is, therefore, expected to yield the most accurate results of the three functionals employed. The hybrid B3LYP functional is by far the most popular functional, representing about 80% of the total occurrences of density functionals in the literature over 1990–2006 [40], and it is, therefore, desirable to compare its performance to the more elaborate M05-2X functional. BLYP is a gradient-corrected nonhybrid functional, and therefore the least expensive computationally.

The formation energies were corrected for basis set superposition error (BSSE) using the counterpoise (CP) procedure [45]. The CP-corrected formation energy of a cluster BWn (B ≡ U(keto), U(enol), 5BrU(keto) or 5BrU(enol); W ≡ water; $n = 50$ or 100) follows from:

$$\Delta E_{\mathrm{BWn}}^{\mathrm{CP}} = E_{\mathrm{BWn}}^{\{\mathrm{BWn}\}}(\mathrm{BWn}) - E_{\mathrm{B}}^{\{\mathrm{BWn}\}}(\mathrm{BWn})$$
$$- \sum_{i=1}^{n} E_{\mathrm{W}_i}^{\{\mathrm{BWn}\}}(\mathrm{BWn}) + E_{\mathrm{B}}^{\mathrm{def}} + E_{\mathrm{W}}^{\mathrm{def}} + \Delta E_{\mathrm{keto}\rightarrow\mathrm{enol}}^{\mathrm{gas}}$$
(1)

where $E_{\mathrm{B}}^{\mathrm{def}}$ is the base deformation energy, corresponding to the energy required to bring the base from its equilibrium geometry to the geometry it adopts in the complex, and $\Delta E_{\mathrm{W}}^{\mathrm{def}}$ is the sum of the water deformation energies:

$$E_{\mathrm{X}}^{\mathrm{def}} = E_{\mathrm{X}}^{\{\mathrm{X}\}}(\mathrm{BWn}) - E_{\mathrm{X}}^{\{\mathrm{X}\}}(\mathrm{X}) \quad \mathrm{X} = \mathrm{B} \text{ or } \mathrm{W}_i \quad (2)$$

$$E_{\mathrm{W}}^{\mathrm{def}} = \sum_{i=1}^{n} E_{\mathrm{W}_i}^{\mathrm{def}} \quad (3)$$

The subscripts indicate the molecular system; the superscripts (in curly brackets) indicate the basis set used in the energy evaluation, i.e., the basis set of the base, {B}, the basis set of a water molecule, {W_i}, or the basis set of the entire system, {BWn}; in round brackets is indicated whether the calculation is done at the optimized geometry of the entire system (BWn), or at the monomer-optimized geometry (X). $\Delta E_{\mathrm{keto}\rightarrow\mathrm{enol}}^{\mathrm{gas}}$ accounts for the gas-phase stability difference of the keto and enol forms of the base:

$$\Delta E_{\mathrm{keto}\rightarrow\mathrm{enol}}^{\mathrm{gas}} = E_{\mathrm{B}}^{\{\mathrm{B}\}}(\mathrm{B}) - E_{\mathrm{B(keto)}}^{\{\mathrm{B}\}}(\mathrm{B(keto)}) \quad (4)$$

Note that this energy quantity is zero for the keto tautomer, i.e., when B = U(keto) or 5BrU(keto), and only has a nonzero value when B = U(enol) or 5BrU(enol).

Valiron and Mayer [46] argued that the counterpoise scheme described above does not account for so-called higher-order BSSE effects, and proposed a hierarchical counterpoise scheme for N-body clusters. However, Salvador and Szczęśniak [47] found that the two counterpoise schemes lead to very similar results of the counterpoise correction for the hydrogen fluoride trimer and tetramer, and concluded that the conventional scheme is preferred due to the significant extra computational cost required for the hierarchical counterpoise scheme.

In our previous letter on the tautomerization of hydrated uracil and 5-bromouracil [22], $\Delta E^{\mathrm{gas}}(\mathrm{keto}\rightarrow\mathrm{enol})$ was absorbed into the base deformation energy term. Also note that we have computed the energies required to compute the formation energies using Gaussian's "tight" convergence criteria for the self-consistent field (SCF) procedure, with the result that there are some small differences between the values presented in the current work and those reported in Ref. [22].

2.3 Decomposition of the formation energies

In previous work [19, 20, 22], the formation energy was split into two contributions: the base–water interaction energy, describing the interaction between the base B and the water cluster Wn, and the water–water interaction, corresponding to the formation energy of the water cluster, at the geometry of the BWn complex. The base and water deformation energies were included in the base–water and water–water interaction energies, respectively, so that the sum of the water–water and base–water interaction energies was identical to the CP-corrected formation energy of the BWn complex. In the current paper, we do not incorporate the deformation energies in the base–water and water–water interaction energies, but consider them separately. This allows us to discuss the individual contributions to the tautomerization energies. The formation energy can then be decomposed according to the following equation:

$$\Delta_{\mathrm{BWn}}^{\mathrm{CP}} = \Delta E_{\mathrm{B-(Wn)}}^{\mathrm{CP}} + \Delta E_{\mathrm{Wn}}^{\mathrm{CP}} + E_{\mathrm{B}}^{\mathrm{def}} + E_{\mathrm{W}}^{\mathrm{def}} + \Delta E_{\mathrm{keto}\rightarrow\mathrm{enol}}^{\mathrm{gas}}$$
(5)

The base–water interaction energy follows from:

$$\Delta E_{\mathrm{B-(Wn)}}^{\mathrm{CP}} = E_{\mathrm{BWn}}^{\{\mathrm{BWn}\}}(\mathrm{BWn}) - E_{\mathrm{B}}^{\{\mathrm{BWn}\}}(\mathrm{BWn})$$
$$- E_{\mathrm{(Wn)}}^{\{\mathrm{BWn}\}}(\mathrm{BWn}) \quad (6)$$

whereas the water–water interaction follows from:

$$\Delta E_{\text{Wn}}^{\text{CP}} = E_{(\text{Wn})}^{\{\text{BWn}\}}(\text{BWn}) - \sum_{i=1}^{n} E_{\text{W}_i}^{\{\text{BWn}\}}(\text{BWn}) \qquad (7)$$

Note that calculating the contributions to the formation energy requires $2n + 4$ energy evaluations ($n = 50$ or 100) for each of the four different bases: the calculation of the complex energy, $E_{\text{BWn}}^{\{\text{BWn}\}}(\text{BWn})$; the calculation of the energy of the water cluster in the complex basis set, $E_{(\text{Wn})}^{\{\text{BWn}\}}(\text{BWn})$; the calculation of the energy of the base in its own basis set, $E_{\text{B}}^{\{\text{B}\}}(\text{BWn})$, and in the complex basis set, $E_{\text{B}}^{\{\text{BWn}\}}(\text{BWn})$; and n calculations of the energy of a water molecule in its own basis set, $E_{\text{W}_i}^{\{\text{W}_i\}}(\text{BWn})$, and in the complex basis set, $E_{\text{W}_i}^{\{\text{BWn}\}}(\text{BWn})$. In addition, the energies of the optimized bases and an optimized water molecule, $E_{\text{B}}^{\{\text{B}\}}(\text{B})$ and $E_{\text{W}_i}^{\{\text{W}_i\}}(\text{W}_i)$ are required. All calculations described in Sects. 2.2 and 2.3 were done with Gaussian 03 [37] and used the "tight" convergence criteria for the self-consistent field procedure.

2.4 Calculation of tautomerization energies

The keto $\rightarrow$ enol tautomerization energies were computed as the difference between the formation energies of the enol and keto forms of U-Wn or 5BrU-Wn. Like the formation energies, the tautomerization energies can be decomposed into individual energy contributions (i.e., contributions from the base and water deformation, base–water and water–water interaction and gas-phase tautomerization energy):

$$\Delta E_{\text{keto}\rightarrow\text{enol}} = \Delta E_{\text{B}}^{\text{def}} + \Delta E_{\text{W}}^{\text{def}} + \Delta\Delta E_{\text{B}-(\text{Wn})} + \Delta\Delta E_{(\text{Wn})} + \Delta E_{\text{keto}\rightarrow\text{enol}}^{\text{gas}} \qquad (8)$$

3 Results

3.1 Tautomerization energies

The tautomerization energies are given in Table 1. It can be seen that the gas-phase tautomerization energies are all positive, and very similar in magnitude (between 45 and 50 kJ/mol) for U and 5BrU, in agreement with earlier studies [7, 8, 12, 14–16]. The gas-phase tautomerization energies computed with the various DFT methods are also in good agreement with Placenza and Grimme's QCISD(T) value of 46.4 kJ/mol [8]. In contrast to the gas-phase results, the tautomerization energies are positive for hydrated U, but negative for hydrated 5BrU, for all methods and for both cluster sizes employed. Thus, hydration reverses the tautomeric preference of 5BrU, rendering the rare tautomeric form to be preferred over the canonical form.

For the complexes hydrated by 50 water molecules, the largest contribution to the tautomerization energies comes from the change in the base–water interaction from the keto to the enol form, favoring the enol form over the keto form for both U and 5BrU. The $\Delta\Delta E_{\text{B}-(\text{Wn})}^{\text{CP}}$ values are more negative for U than for 5BrU; nevertheless, U prefers the keto tautomer. Table 1 shows that this is to a large extent due to $\Delta\Delta E_{\text{Wn}}^{\text{CP}}$, which favors the keto form of U. In contrast, for 5BrU this energy quantity is negative, reinforcing the preference for the enol tautomer. These results indicate that, in the 50-water clusters, the preference of 5BrU for the enol tautomer is largely due to the favorable change in the water–water interaction from the keto to the enol tautomer for this base.

For the complexes hydrated by 100 water molecules the relative importance of the contributions to the tautomerization energies is somewhat different. Also for these complexes the base–water interaction favors the enol form of both U and 5BrU. However, the preference for the enol form is now much larger for 5BrU than for U. Like for the 50-water complexes, in the larger clusters the water–water interaction favors the keto form of U, whereas it favors the enol form of 5BrU. The differences in the water–water interaction are, however, much smaller than for the 50-water complexes. For U, the base–water preference for the enol tautomer is largely cancelled by the water–water preference for the keto tautomer, and the tautomerization energies of hydrated U are similar to the corresponding gas-phase values. For 5BrU, on the other hand, both the base–water and water–water interactions favor the enol tautomer. Thus, the main cause of the different tautomeric preferences of U and 5BrU appears to be due to the differences in the contributions from both the water–water and the base–water interaction.

The formation energies of the bases hydrated by 50 and 100 water molecules, as well as their energy components, are shown in Tables 2 and 3, respectively. The water–water interaction per water molecule, shown in the column labeled $\Delta E_{\text{Wn}}^{\text{CP}}/n$, is slightly larger in the 100-water clusters (by up to ~ 5 kJ/mol), irrespective of whether the water deformation energies are included in the water–water interaction energy. In contrast, the base–water interaction energies are generally smaller in the larger clusters (except in some cases for the keto form of U). This indicates that the waters can form a more efficient water structure in the larger clusters; the formation of this more efficient water network appears to be energetically preferred over positioning the water molecules such that the water–base interactions are maximized.

The M05-2X base–water and water–water interaction energies, as well as the M05-2X formation energies are larger than the corresponding BLYP and B3LYP results (see Tables 2, 3). This is likely due to the better description

Table 1 Tautomerization energies and their contributions for the complexes of the base interacting with 50 and 100 water molecules computed at different levels of theory

	System	$\Delta E_{\mathrm{B}}^{\mathrm{def}}$	$\Delta E_{\mathrm{W}}^{\mathrm{def}}$	$\Delta\Delta E_{\mathrm{B-(Wn)}}^{\mathrm{CP}}$	$\Delta\Delta E_{\mathrm{Wn}}^{\mathrm{CP}}$	$\Delta E_{\mathrm{keto\to enol}}^{\mathrm{gas}}$	$\Delta E_{\mathrm{keto\to enol}}$
B-W50							
BLYP/6-31G(d,p) optimized structures							
BLYP/6-31G(d,p)	U-W50	27.7	15.1	−124.7	38.9	50.5	7.6
	5BrU-W50	6.2	18.3	−75.6	−61.7	51.4	−61.4
M05-2X/6-31G(d,p)	U-W50	33.5	22.3	−108.8	38.0	44.7	29.6
	5BrU-W50	8.7	32.9	−59.6	−43.3	47.6	−13.7
B3LYP/6-31G(d,p) optimized structures							
B3LYP/6-31G(d,p)	U-W50	23.2	10.8	−111.4	42.5	50.9[a]	16.1
	5BrU-W50	4.5	12.6	−71.1	−54.2	52.5[a]	−55.7
B3LYP/6-31++G(d,p)	U-W50	21.7	12.2	−103.2	39.6	49.9	20.3
	5BrU-W50	3.0	14.3	−65.2	−45.8	48.5	−45.2
M05-2X/6-31G(d,p)	U-W50	25.3	12.8	−94.2	44.6	44.7	33.2
	5BrU-W50	5.1	17.1	−53.0	−30.9	47.6	−14.0
B-W100							
BLYP/6-31G(d,p) optimized structures							
BLYP/6-31G(d,p)	U-W100	0.3	1.9	−13.3	26.5	50.5	65.9
	5BrU-W100	0.6	−3.9	−48.6	−5.5	51.4	−6.0
M05-2X/6-31G(d,p)	U-W100	−0.3	3.3	−26.6	30.9	44.7	52.1
	5BrU-W100	−0.5	−0.8	−46.2	−14.7	47.6	−14.6
B3LYP/6-31G(d,p) optimized structures							
BLYP/6-31G(d,p)	U-W100	1.2	11.7	−13.0	4.8	50.5	55.2
	5BrU-W100	19.0	2.3	−93.9	−22.7	51.4	−44.0
B3LYP/6-31G(d,p)	U-W100	1.1	17.3	−16.3	3.3	50.9	56.3
	5BrU-W100	21.6	6.5	−94.6	−22.5	52.5	−36.5
M05-2X/6-31G(d,p)	U-W100	1.9	21.0	−27.7	−1.0	44.7	38.9
	5BrU-W100	22.8	8.8	−96.6	−1.5	47.6	−18.7

Energies in kJ/mol

[a] Reference [22] erroneously lists the U-W50 and 5BrU-W50 $\Delta E_{\mathrm{keto\to enol}}^{\mathrm{gas}}$ values as 49.9 and 48.5 kJ/mol, respectively, which are the B3LYP/6-31++G(d,p) values

of the intermolecular interactions (and particularly, the description of the dispersion interaction) by the M05-2X functional. Trends in the different contributions to the formation energies and tautomerization energies are, in general, similar for the three functionals employed.

3.2 The water network in the 50- and 100-water clusters

To attempt to explain the different magnitudes of the energy contributions in the 50- and 100-water clusters we compared the water network in the different clusters. The distribution of the water molecules in layers around the central base in the complexes optimized with B3LYP/6-31G(d,p) is shown in Table 4. The layers were defined by spheres with their centers coinciding with the geometric center of the base. A comparison of the water distribution in the B-W50 and B-W100 clusters reveals that the smaller clusters (except the enol 5BrU cluster) contain more water molecules in the 5–6 Å layer than the 100-water clusters. Similarly, summing the water molecules in the layers nearest the central base shows that the smaller clusters (again except the enol 5BrU cluster) contain more water molecules within 6 Å of the geometric center of the base. Note that the U(enol)-W100 cluster contains five more water molecules in the 0–4 Å layer than the U(enol)-W50 cluster. However, this just reflects some water molecules close to the 4-Å boundary in these clusters, as can be deduced from the larger number of water molecules in the 4–5-Å layer in the U(enol)-W50 cluster. In line with the clusters of the other hydrated bases (except the enol 5BrU cluster), the U(enol)-W50 cluster contains three more water molecules within 6 Å of the base than the U(enol)-W100 cluster. A comparison of the B-W50 and B-W100 results of the B3LYP/6-31G(d,p) optimized complexes (Tables 2, 3) shows that the base–water interaction energy is more

Table 2 The formation energies and their components of the keto and enol tautomeric forms of the U-W50 and 5BrU-W50 systems computed at different levels of theory

Level of theory	System	$E_{\mathrm{B}}^{\mathrm{def}}$	$E_{\mathrm{W}}^{\mathrm{def}}$	$\Delta E_{\mathrm{B-(Wn)}}^{\mathrm{CP}}$	$\Delta E_{\mathrm{Wn}}^{\mathrm{CP}}/n$	$\Delta E_{\mathrm{keto\to enol}}^{\mathrm{gas}}$	$\Delta E_{\mathrm{BWn}}^{\mathrm{CP}}$
BLYP/6-31G(d,p) optimized structures							
BLYP/6-31G(d,p)	U(keto)-W50	21.9	176.2	−142.8	−45.7	0.0	−2,230.7
	U(enol)-W50	49.6	191.4	−267.5	−44.9	50.5	−2,223.1
	5BrU(keto)-W50	33.6	179.6	−150.2	−43.7	0.0	−2,121.2
	5BrU(enol)-W50	39.8	197.8	−225.8	−44.9	51.4	−2,182.6
M05-2X/6-31G(d,p)	U(keto)-W50	33.9	397.9	−255.8	−53.5	0.0	−2,500.7
	U(enol)-W50	67.5	420.2	−364.7	−52.8	44.7	−2,471.1
	5BrU(keto)-W50	49.2	390.9	−280.8	−51.6	0.0	−2,420.9
	5BrU(enol)-W50	57.9	423.7	−340.4	−52.5	47.6	−2,434.6
B3LYP/6-31G(d,p) optimized structures							
B3LYP/6-31G(d,p)	U(keto)-W50	20.3	138.9	−169.5	−46.9	0.0	−2,356.0
	U(enol)-W50	43.5	149.8	−280.8	−46.1	50.9	−2,339.9
	5BrU(keto)-W50	28.1	139.8	−169.9	−44.9	0.0	−2,245.2
	5BrU(enol)-W50	32.6	152.4	−241.0	−45.9	52.5	−2,300.8
B3LYP/6-31++G(d,p)	U(keto)-W50	17.5	122.6	−149.2	−40.1	0.0	−2,011.9
	U(enol)-W50	39.2	134.7	−252.4	−39.3	49.9	−1,991.6
	5BrU(keto)-W50	26.8	120.4	−146.6	−38.4	0.0	−1,918.1
	5BrU(enol)-W50	29.8	134.7	−211.8	−39.3	48.5	−1,963.3
M05-2X/6-31G(d,p)	U(keto)-W50	21.7	189.9	−250.5	−51.0	0.0	−2,589.9
	U(enol)-W50	47.0	202.6	−344.7	−50.1	44.7	−2,556.8
	5BrU(keto)-W50	30.4	186.8	−268.3	−49.2	0.0	−2,511.1
	5BrU(enol)-W50	35.5	203.8	−321.3	−49.8	47.6	−2,525.2

Energies in kJ/mol

favorable in the 50-water clusters than in the 100-water clusters for all bases except the keto form of uracil. (This result does not change if the base deformation energies are included in the base–water interaction energies.) It seems likely that the larger base–water interaction in the smaller clusters results from the larger number of water molecules near the central base.

In both cluster sizes, the water structure around the enol tautomer of 5BrU stretches further from the base as compared to the other bases. The 50-water cluster of the enol form of 5BrU is the only one of the small clusters with two water molecules beyond the 9-Å boundary, whereas the 100-water cluster of this base is the only of the large clusters with one water beyond the 10-Å border.

The total number of water–water H-bonds is surprisingly similar for the different bases; it ranges from 79 for 5BrU(enol) to 81 for U(keto) in the 50-water clusters and from 172 for U(enol) to 175 for BrU(keto) in the 100-water clusters (see Table 4). There is some correlation between the number of water–water H-bonds and the water–water interaction energy: U(keto) has the highest number of water–water H-bonds and the largest water–water interaction energy in the 50-water clusters, whereas in the 100-water clusters this is the case for the two brominated bases.

However, there is no ultimate relationship between the number of water–water H-bonds and the magnitude of the water–water interaction. For example, the 50-water cluster with the smallest number of water–water H-bonds, 5BrU(enol)-W50, does not have the smallest water–water interaction energy. As the total number of water–water H-bonds is so similar in the different clusters, other effects, like the strength of the individual H-bonds and differences in H-bond cooperativity, may affect the relative magnitudes of the water–water interaction energy. This makes it much more difficult to relate the magnitude of the water–water interaction to simple measures such as the number of H-bonds. The water–water interaction decreases from U(keto) to U(enol) but increases from 5BrU(keto) to 5BrU(enol) for both cluster sizes and all methods employed (except M05-2X for the 100-water clusters), confirming the importance of the water–water interaction for an understanding of the different tautomeric shifts of U and 5BrU.

3.3 Comparison of the brominated and nonbrominated bases

Two main trends can be observed in the base–water interaction energies (Tables 2, 3): (1) they increase from

Table 3 The formation energies and their components of the keto and enol tautomeric forms of the U-W100 and 5BrU-W100 systems computed at different levels of theory

Level of theory	System	E_B^{def}	E_W^{def}	$\Delta E_{B-(Wn)}^{CP}$	$\Delta E_{Wn}^{CP}/n$	$\Delta E_{keto\to enol}^{gas}$	ΔE_{BWn}^{CP}
BLYP/6-31G(d,p) optimized structures							
BLYP/6-31G(d,p)	U(keto)-W100	4.1	241.5	−134.5	−48.1	0.0	−4,694.0
	U(enol)-W100	4.4	243.3	−147.8	−47.8	50.5	−4,628.1
	5BrU(keto)-W100	4.8	245.5	−84.0	−48.0	0.0	−4,636.9
	5BrU(enol)-W100	5.3	241.6	−132.6	−48.1	51.4	−4,643.0
M05-2X/6-31G(d,p)	U(keto)-W100	2.2	591.4	−212.6	−55.6	0.0	−5,178.9
	U(enol)-W100	1.9	594.7	−239.2	−55.3	44.7	−5,126.9
	5BrU(keto)-W100	2.5	591.1	−179.7	−55.5	0.0	−5,133.1
	5BrU(enol)-W100	2.0	590.3	−225.9	−55.6	47.6	−5,147.7
B3LYP/6-31G(d,p) optimized structures							
BLYP/6-31G(d,p)	U(keto)-W100	29.5	186.1	−165.0	−45.7	0.0	−4,516.9
	U(enol)-W100	30.8	197.8	−178.0	−45.6	50.5	−4,461.7
	5BrU(keto)-W100	22.2	199.6	−75.7	−45.7	0.0	−4,426.8
	5BrU(enol)-W100	41.2	201.9	−169.7	−46.0	51.4	−4,470.8
B3LYP/6-31G(d,p)	U(keto)-W100	27.1	308.2	−197.3	−49.7	0.0	−4,828.0
	U(enol)-W100	28.2	325.5	−213.7	−49.6	50.9	−4,771.7
	5BrU(keto)-W100	18.4	322.1	−111.3	−49.7	0.0	−4,742.8
	5BrU(enol)-W100	40.0	328.6	−205.9	−49.9	52.5	−4,779.3
M05-2X/6-31G(d,p)	U(keto)-W100	28.7	414.0	−268.4	−54.5	0.0	−5,280.0
	U(enol)-W100	30.6	435.0	−296.1	−54.6	44.7	−5,241.1
	5BrU(keto)-W100	20.4	427.2	−203.9	−54.6	0.0	−5,218.4
	5BrU(enol)-W100	43.3	436.0	−300.5	−54.6	47.6	−5,237.1

Energies in kJ/mol

the keto to the enol form for both U and 5BrU and (2) they tend to be smaller for the brominated bases, particularly for the enol form (this trend is even clearer when the base–water deformation energy is summed into the base–water interaction energy). As a result, the enol form of uracil has the largest base–water interaction energy.

The bromine atom in the brominated bases is positioned at the hydrophobic side of uracil (i.e., there are no water molecules interacting with the 5-hydrogen in uracil). This suggests the possibility of forming halogen bonds, which have been proposed as potentially stabilizing interactions in biological molecules [48]. It has been shown that halogens can form two kinds of stabilizing interactions with water: proper halogen bonds ($X \cdots O_w$; where X is the halogen and O_w is a water oxygen) and halogen–hydrogen interactions ($X \cdots H_w$). Note, however, that the substitution of the hydrogen in the 5-position by a bromine atom generally reduces the base–water interaction energy (Tables 2, 3), and the overall interaction between the bromine and the water molecules, therefore, does not seem to be favorable. However, we are interested in the differences between the keto and enol forms, which may be influenced by halogen–water interactions. Figures 3 and 4 show the water molecules that bind to the central base in the 50 and 100-water clusters,

respectively, as well as the water molecules that are in close proximity to the bromine. In the 50-water clusters of the U and 5BrU enol tautomers the hydroxyl group is incorporated into a cooperative water chain, where the OH-group functions as a water molecule. The waters close to the bromine do not seem to interact directly with the halogen atom, but form a water chain around it. In the cluster of the keto tautomer of 5BrU, the water molecule at the end of this chain (indicated by an arrow in Fig. 3) appears to form a halogen–hydrogen interaction [$R(Br \cdots H_w) = 2.80$ Å; $\angle(Br \cdots H_w O_w = 143°)$], but the orientation of the other water molecules seems to be mainly determined by the formation of a favorable water network in the cluster. The larger base–water interaction energy in the enol tautomers of U and 5BrU is presumably mainly caused by the favorable water structure formed around the hydroxyl group. Bromine–water contacts do not seem to contribute to the preference for the enol tautomer; if anything, they decrease it. Note that the base–water preference for the enol form is larger for U than 5BrU (Table 1).

In the 100-water cluster of the keto tautomer of 5BrU, there appears to be one water molecule with a possible halogen–hydrogen interaction ($R(Br \cdots H_w) = 2.54$ Å; $\angle(Br \cdots H_w O_w = 133°)$; the hydrogen pointing to the

Table 4 Distribution of the water molecules in layers around the central base in the B3LYP/6-31G(d,p) optimized complexes

Layer[a]	B-W50				B-W100			
	U(keto)	U(enol)	5BrU(keto)	5BrU(enol)	U(keto)	U(enol)	5BrU(keto)	5BrU(enol)
0–4	4	3	4	3	4	8	3	4
4–5	14	13	13	15	12	9	14	10
5–6	16	14	16	8	12	10	10	14
6–7	10	13	12	15	21	22	27	21
7–8	6	7	5	7	25	30	20	24
8–9	0	0	0	2	21	18	21	13
9–10	0	0	0	0	5	3	5	13
b–w[b]	6	7	7	7	8	8	6	5
w–w[c]	81	80	80	79	173	172	175	175
Br–w[d]	–	–	6	4	–	–	4	6

The total number of base–water, water–water and halogen contacts are shown as well

[a] The inner and outer boundaries of the $n1$–$n2$ layer are defined by two spheres with radius $n1$ and $n2$ Å, respectively, with the center of the spheres coinciding with the geometric center of the base. A water molecule was considered to be in the layer when its geometric center fell within the $n1$ and $n2$ boundaries

[b] Number of base–water H-bonds

[c] Number of water–water H-bonds in the B3LYP/6-31G(d,p) optimized complexes

[d] Number halogen contacts close to the bromine. An X–H···O (X = C, N, O) interaction was considered to be a H-bond if R(O···H) <2.3 Å and ∠(XH···O) >90°. Halogen contacts were counted if either R(Br···O) <3.37 Å (the sum of the Br and O van der Waals radii) or R(Br···H) <3.05 (the sum of the Br and O van der Waals radii). Those that are considered proper halogen bonds or halogen–hydrogen interactions are indicated by arrows in Figs. 3 and 4
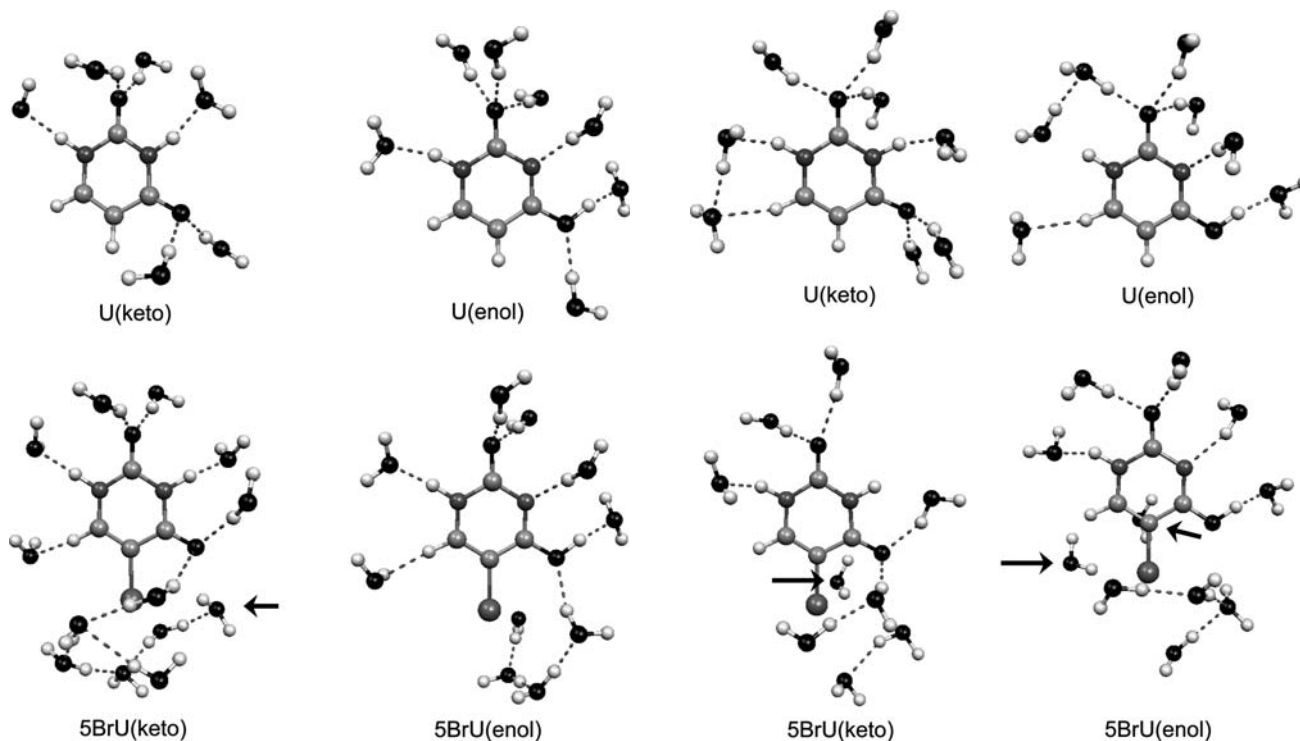

Fig. 3 Fragments of the B3LYP/6-31G(d,p) optimized structures of the keto and enol tautomers of U-(H$_2$O)$_{50}$ and 5BrU-(H$_2$O)$_{50}$ showing the water molecules that form H-bonds with the base as well as the water molecules that are within van der Waals distance of the bromine atom [R(Br···O) <3.37 Å or R(Br···H) <3.05 Å]. Water molecules that form halogen–hydrogen interactions are identified by *arrows*

Fig. 4 Fragments of the B3LYP/6-31G(d,p) optimized structures of the keto and enol tautomers of U-(H$_2$O)$_{100}$ and 5BrU-(H$_2$O)$_{100}$ showing the water molecules that form H-bonds with the base as well as the water molecules that are within van der Waals distance of the bromine atom [R(Br···O) <3.37 Å or R(Br···H) <3.05 Å]. Water molecules that form halogen–hydrogen interactions are identified by *arrows*

bromine is not H-bonding to other water molecules in the cluster). In the cluster of the enol tautomer, there are two water molecules with clear halogen–hydrogen contacts $(R(Br \cdots H_w) = 2.39$ Å; $\angle(Br \cdots H_w O_w = 168°;$ $R(Br \cdots H_w) = 2.57$ Å; $\angle(Br \cdots H_w O_w = 153°)$. Both waters also take part in the H-bonding water network, but one of their hydrogens points to the bromine and does not H-bond with other water molecules. It is likely that these halogen–hydrogen interactions enhance the hydrogen bonding in the water network. Thus, the larger base–water interaction in the enol form of 5BrU may at least partially be rationalized with the increase in the strength of the water network due to halogen–hydrogen interactions.

Hu et al. [12, 17] suggested that the bromine substitution at position 5 of U may make it more difficult for water molecules to enter the "S2" region (the space defined by lines through the C5–H and C4=O bonds), which would lead to the loss of protection induced by water molecules in this region. Our optimized structures do not show any evidence for this mechanism; there are no more water molecules in the S2 region in U than in 5BrU. In addition, the S2 water molecules in U do not show the hydrogen-bonded chain linking C5–H and C4=O as observed in the U-Wn ($n = 1$–3) structures optimized by Hu et al., presumably because of competing interactions with water molecules within the larger water network in the U-W50 and U-W100 clusters.

4 Discussion and conclusion

We have studied the canonical (keto) and rare (enol) tautomers of U and 5BrU in clusters consisting of 50 and 100 water molecules, optimized at two different levels of theory, BLYP/6-31G(d,p) and B3LYP/6-31G(d,p). Tautomerization energies were computed using the BLYP, B3LYP and M05-2X density functionals. For all four sets of clusters (BLYP or B3LYP optimized, containing 50 or 100 water clusters) and at all levels of theory, the keto form of U is favored over the enol tautomer, whereas this preference is reversed for 5BrU. In contrast, the gas-phase tautomerization energies of U and 5BrU are very similar, favoring the keto tautomer.

These results differ from previous studies using continuum solvation models [14, 15], which found that for both U and 5BrU the keto tautomer is favored in bulk water. Our results show that the water–water interactions in the water network play an important role in determining the tautomeric preferences of U and 5BrU. It is, therefore, likely that the inclusion of explicit water–water interactions, which are lacking in continuum solvation models, is required to correctly describe these effects. Recently, Palafox et al. [49] studied the first hydration shell of two

thymidine nucleosides using MP2 and DFT, and found that Tomasi's polarized continuum model (PCM) of solvation [50–55] considerably underestimates the deformation of the structure by the water molecules. Thus, the need for explicit waters may be even more important when considering larger, more flexible, DNA moieties. Suhai, Jalkanen and others [56–62] have demonstrated the requirement for explicit water molecules to reproduce and interpret vibration absorption (VA), vibrational circular dichroism (VCD), Raman and Raman optical activity (ROA) spectra of the alanine dipeptide in aqueous solution. Experimental NMR data verified that explicit water molecules are essential to stabilize alanine dipeptide structures that are not stable in the gas phase [63, 64]. Similarly, explicit water molecules are needed to stabilize the zwitterionic form of the L-alanine amino acid, which is not stable in the gas phase or in a continuum solvent, and to capture the main VCD features of methyl lactate in water [65]. In view of the failure of continuum solvation models in these examples as well as in the current study, we advocate the use of explicit water models or combined explicit/continuum solvation models for the study of biomolecules in aqueous solution.

Note that the MC results obtained by Orozco et al. [14] and by us predict the 5BrU keto form to be favored over the enol form, in disagreement with our DFT results. However, this is likely due to the use of semiempirical potential functions in the MC simulations, which do not account for effects like polarization and water monomer deformation during geometry optimization of the system.

The different contributions to the tautomerization energies are of varying importance in the two differently-sized clusters. In the 50-water clusters, the preference of 5BrU for the enol tautomer is largely due to the more favorable water–water interactions in the cluster around the brominated base, whereas in the 100-water clusters the different tautomeric preferences of U and 5BrU are due to differences in the contributions from both the water–water and the base–water interaction. The 50-water clusters show a favorable cooperative coordination of water molecules around the hydroxyl group in the U and 5BrU enol tautomers, leading to an increased base–water interaction energy, whereas in the 100-water clusters the larger base–water interaction in the enol form of 5BrU may result from the increased strength of the water network due to halogen–hydrogen interactions. In both cluster sizes, the water structure around the enol tautomer of 5BrU stretches further from the base as compared to the other bases. It, therefore, appears that differences in the water structure around the base are (at least partially) responsible for the favorable tautomeric shift of hydrated 5BrU. We propose that the preference for the rare tautomeric form of 5BrU is due to the more efficient incorporation of the hydroxyl

group in the water network as compared to the carbonyl group, with additional stabilization of the water shell by halogen interactions.

The water molecules that bind directly to uracil form only one H-bond with the base. None of the water molecules show the binding patterns observed in mono and dihydrated uracil clusters, namely a water molecule forming two H-bonds to the base or a water dimer bridging different functional groups [7, 12, 16, 66–77]. When more water molecules are present, they prefer to form small clusters [19, 20, 71, 75], indicating that water–water interactions are energetically more favorable than base–water interactions. Thus, the orientations and positions of the water molecules in the clusters studied in the present work are probably mainly determined by the drive to form a strong H-bond network in the water shell. This appears to guide the water molecules away from the optimal water binding sites of uracil. The lack of the strongly bound water molecules observed in microhydrated clusters counters Hu et al.'s [12, 17] hypothesis of the protective effect of water molecules in the S1 binding region.

Our findings do not prove that the mutagenic activity of 5-bromouradine is due to the preference of 5BrU for the rare enol tautomeric form. In nucleic acids uracil does not occur in its isolated form, but is connected to a sugar moiety via its N1 atom. This may have influence on the water structure surrounding the base, and therefore on the relative stabilities of the different tautomers of U and 5BrU. Entropic effects may also have some effect on the results, though we do not expect these to reverse the main conclusion of the current work. This is supported by previous work by Hobza et al. [15, 78] which established that entropy does not significantly affect the relative stability of the tautomers of U and 5BrU. In addition, Orozco et al. [14] found that entropic effects play only a minor role in the keto-enol tautomerism. Hu et al. [79] found that the presence of Na^+ ions affects the tautomerization of U and 5BrU; so metal cations may also have to be taken into account. Another issue to be kept in mind is that all clusters considered have a very large number of local minima (resulting from variations in the coordination of the water molecules around the base), whereas we only considered one local minimum on each of the potential energy surfaces. Ideally, one would use averaged relative stabilities obtained from ab initio molecular dynamics simulations on nucleosides (or larger DNA fragments) surrounded by a large number of explicit water molecules, carried out at body temperature. Such calculations are not feasible computationally on today's computer hardware. The limited number of local minima used in the current study, imposed by the computational expense of the geometry optimizations, introduces some uncertainty in the conclusions reached. However, we stress that despite these apparent approximations, all calculations on all different sets of geometries employed (BLYP or B3LYP optimized, containing 50 or 100 water molecules) give the result that a bromine atom in the 5-position considerably increases the proportion of the hydroxyl form present in uracil. Our results indicate that, at present, the tautomeric mechanism cannot be ruled out as an explanation of the mutagenic activity of 5BrU.

References

1. Watson JD, Crick FHC (1953) Nature 171:737–738
2. Topal MD, Fresco JR (1976) Nature 263:285–289
3. Les A, Adamowicz J (1989) J Phys Chem 93:7078–7081
4. Estrin DA, Paglieri L, Corongiu G (1994) J Phys Chem 98:5653–5660
5. Paglieri L, Corongiu G, Estrin DA (1995) Int J Quant Chem 56:615–625
6. Nguyen MT, Chandra AK, Zeegers-Huyskens T (1998) J Chem Soc Faraday Trans 94:1277
7. Kryachko ES, Nguyen MT, Zeegers-Huyskens T (2001) J Phys Chem A 105:1288–1295
8. Piacenza M, Grimme S (2004) J Comput Chem 25:83–98
9. Bakker JM, Sinha RK, Besson T, Brugnara M, Tosi P, Salpin J-Y, Maître P (2008) J Phys Chem A 112:12393–12400
10. Freese E (1959) J Mol Biol 1:87–105
11. Katritzky AR, Waring AJ (1962) J Chem Soc 1540
12. Hu X, Li H, Ding J, Han S (2004) Biochemistry 43:6361–6369
13. Yu H, Eritja R, Bloom JB, Goodman MF (1993) J Biol Chem 268:15935–15943
14. Orozco M, Hernández A, Luque FJ (1998) J Phys Chem A 102:5228–5233
15. Hanus M, Kabeláč M, Nachtigallová D, Hobza P (2005) Biochemistry 44:1701–1707
16. Kabeláč M, Hobza P (2007) Phys Chem Chem Phys 9:903–917
17. Hu X, Li H, Liang W, Han S (2004) J Phys Chem B 108:12999–13007
18. Kurita N, Danilov VI, Anisimov VM, Hovorun D, Nakatsu T, Dedachi K (2007) J Mol Struct Dyn 24:665–665 (Book of Abstracts, Albany 2007: The Conversation 15, 19–23 Jun 2007)
19. Danilov VI, van Mourik T, Poltev VI (2006) Chem Phys Lett 429:255–260
20. van Mourik T, Danilov VI, Gonzales E, Deriabina A, Poltev VI (2007) Chem Phys Lett 445:305–308
21. Sykes MT, Levitt M (2007) PNAS 104:12336–12340
22. Danilov VI, van Mourik T, Kurita N, Wakabayashi H, Tsukamoto T, Hovorun DM (2009) J Phys Chem A 113:2233–2235
23. Degtyarenko IM, Jalkanen KJ, Gurtovenko AA, Nieminen RM (2007) J Phys Chem B 111:4227–4234
24. Becke AD (1988) Phys Rev A 38:3098–3100
25. Lee C, Yang W, Parr RG (1988) Phys Rev B 37:785–789
26. Becke AD (1993) J Chem Phys 98:5648–5652
27. Stephens PJ, Devlin FJ, Chabalowski CF, Frisch MJ (1994) J Phys Chem 98:11623–11627
28. Metropolis N, Rosenbluth AW, Rosenbluth MN, Teller AH, Teller E (1953) J Chem Phys 21:1087–1092

29. Lee JK, Barker JA, Abraham FF (1973) J Chem Phys 58:3166–3180
30. Mruzik MR, Abraham FF, Schreiber DE, Pound GM (1976) J Chem Phys 64:481–491
31. González-Jiménez E, Castro-Valdez I, López-Apresa E, Filippov SV, Teplukhin AV, Poltev VI (1999) J Mol Struct 493:301–308
32. González E, Cedeño FI, Teplukhin AV, Malenkov GG, Poltev VI (2000) Rev Mex Fis 46:142–147
33. Poltev VI, Deryabina AS, González E, Grokhlina TI (2002) Biofizika 47:996–1004
34. Delley B (1990) J Chem Phys 92:508–517
35. Benedek NA, Snook IK, Latham K, Yarovsky I (2005) J Chem Phys 122:144102
36. Inada Y, Orita H (2007) J Comput Chem 29:225–232
37. Frisch MJ, Trucks GW, Schlegel HB, Scuseria GE, Robb MA, Cheeseman JR, Montgomery J, J.A., Vreven T, Kudin KN, Burant JC, Millam JM, Iyengar SS, Tomasi J, Barone V, Mennucci B, Cossi M, Scalmani G, Rega N, Petersson GA, Nakatsuji H, Hada M, Ehara M, Toyota K, Fukuda R, Hasegawa J, Ishida M, Nakajima T, Honda Y, Kitao O, Nakai H, Klene M, Li X, Knox JE, Hratchian HP, Cross JB, Adamo C, Jaramillo J, Gomperts R, Stratmann RE, Yazyev O, Austin AJ, Cammi R, Pomelli C, Ochterski JW, Ayala PY, Morokuma K, Voth GA, Salvador P, Dannenberg JJ, Zakrzewski VG, Dapprich S, Daniels AD, Strain MC, Farkas O, Malick DK, Rabuck AD, Raghavachari K, Foresman JB, Ortiz JV, Cui Q, Baboul AG, Clifford S, Cioslowski J, Stefanov BB, Liu G, Liashenko A, Piskorz P, Komaromi I, Martin RL, Fox DJ, Keith T, Al-Laham MA, Peng CY, Nanayakkara A, Challacombe M, Gill PMW, Johnson B, Chen W, Wong MW, Gonzalez C, Pople JA, Gaussian 03, Revision E.01. Gaussian Inc., Wallingford
38. Dahlke EE, Olson RM, Leverentz HR, Truhlar DG (2008) J Phys Chem A 112:3976–3984
39. Zhao Y, Schultz NE, Truhlar DG (2006) J Chem Theor Comput 2:364–382
40. Sousa SF, Fernandes PA, Ramos MJ (2007) J Phys Chem A 111:10439–10452
41. Zhao Y, Truhlar DG (2007) J Chem Theor Comput 3:289–300
42. Leverentz HR, Truhlar DG (2008) J Phys Chem A 112:6009–6016
43. van Mourik T (2008) J Chem Theor Comput 4:1610–1619
44. Zhao Y, Truhlar DG (2008) Acc Chem Res 41:157–167
45. Boys SF, Bernardi F (1970) Mol Phys 19:553–566
46. Valiron P, Mayer I (1997) Chem Phys Lett 275:46–55
47. Salvador P, Szczęśniak MM (2003) J Chem Phys 118:537–549
48. Auffinger P, Hays FA, Westhof E, Ho S (2004) PNAS 101:16789–16794
49. Palafox MA, Iza N, de la Fuente M, Navarro R (2009) J Phys Chem B 113:2458–2476
50. Miertus S, Scrocco E, Tomasi J (1981) Chem Phys 55:117–129
51. Tomasi J, Persico M (1994) Chem Rev 94:2027–2094
52. Cossi M, Barone V, Cammi R, Tomasi J (1996) Chem Phys Lett 255:327–335
53. Amovilli C, Barone V, Cammi R, Cances E, Cossi M, Mennucci B, Pomelli CS, Tomasi J (1999) Adv Quant Chem 32:227
54. Cramer CJ, Truhlar DG (1999) Chem Rev 99:2161–2200
55. Cossi M, Scalmani G, Rega N, Barone V (2002) J Chem Phys 117:43–54
56. Deng Z, Polavarapu PL, Ford SJ, Hecht L, Barron LD, Ewig CS, Jalkanen KJ (1996) J Phys Chem 100:2025–2034
57. Jalkanen KJ, Suhai S (1996) Chem Phys 208:81–116
58. Han W-G, Jalkanen KJ, Elstner M, Suhai S (1998) J Phys Chem B 102:2587–2602
59. Jalkanen KJ, Elstner M, Suhai S (1998) J Mol Struct 675:61–77
60. Bohr H, Jalkanen KJ (2005) Spectroscopic studies of small biomolecules in condensed phases. In: Clark JW, Panoff RM, Li H (eds) Condsensed matter theory. Nova Science Publishers, Hauppage, New York
61. Jalkanen KJ, Degtyarenko IM, Nieminen RM, Cao X, Nafie LA, Zhu F, Barron LD (2008) Theor Chem Acc 119:191–210
62. Mukhopadhyay P, Zuber G, Beratan DN (2008) Biophys J 95:5574–5586
63. Poon C-D, Samulski ET, Weise CF, Weisshaar JC (2000) J Am Chem Soc 122:5642–5643
64. Weise CF, Weisshaar JC (2003) J Phys Chem B 107:3265–3277
65. Losada M, Xu Y (2007) Phys Chem Chem Phys 9:3127–3135
66. Smets J, McCarthy WJ, Adamowicz L (1996) J Phys Chem 100:14655
67. Aamouche A, Berthier G, Cadioli B, Gallinella E, Ghomi M (1998) J Mol Struct 426:307–312
68. Chahinian M, Seba HB, Ancian B (1998) Chem Phys Lett 285:337–345
69. Dolgounitcheva O, Zakrzewski VG, Ortiz JV (1999) J Phys Chem A 103:7912
70. van Mourik T, Price SL, Clary DC (1999) J Phys Chem A 103:1611–1618
71. Gadre SR, Babu K, Rendell AP (2000) J Phys Chem A 104:8976–8982
72. van Mourik T, Benoit DM, Price SL, Clary DC (2000) Phys Chem Chem Phys 2:1281–1290
73. Gaigeot M-P, Ghomi M (2001) J Phys Chem B 105:5007–5017
74. Kryachko E, Nguyen MT, Zeegers-Huyskens T (2001) J Phys Chem A 105:3379–3387
75. van Mourik T (2001) Phys Chem Chem Phys 3:2886–2892
76. van Mourik T, Price SL, Clary DC (2001) Faraday Discuss 118:95–108
77. Casaes RN, Paul JB, McLaughlin P, Saykally RJ, van Mourik T (2004) J Phys Chem A 108:10989–10996
78. Rejnek J, Hanus M, Kabeláč M, Ryjáček F, Hobza P (2005) Phys Chem Chem Phys 7:2006–2017
79. Hu X, Li H, Zhang L, Han S (2007) J Phys Chem B 111:9347–9354